PAPER

Check for updates

Electro-kinetic remediation of chromium-contaminated soil by a three-dimensional electrode coupled with a permeable reactive barrier

Fengjiao Xue,†[a] Yujie Yan,†[a] Ming Xia,†[a] Faheem Muhammad,†[a] Lin Yu,†[ab] Feng Xu,†[d] YanChyuan Shiau,*[c] Dongwei Li ID *[a] and Binquan Jiao*[ab]

Improper disposal of chromium (Cr) and its compounds, especially hexavalent chromium (Cr(vi)), results in soil and ground water pollution and is consequently harmful to human health. In this study, three-dimensional electro-kinetic remediation of Cr-contaminated soil is investigated by coupling a two-dimensional electrode with a permeable reactive barrier (PRB) with a graphite electrode as the third electrode. Mixed zero-valent iron and zeolite are used as filling materials in the PRB. Moreover, three experimental conditions, *i.e.* two-dimensional electro-kinetic remediation with and without PRB and three-dimensional electro-kinetic remediation with PRB, are investigated herein. The results are evaluated based on the removal rate and leaching efficiency both in the pre- and post-experiments. Upon comparing the three conditions, the results show that three-dimensional electro-kinetic remediation with PRB has a better effect on both leaching efficiency and removal rate of contaminated soil. Single and multifactor experiments were designed to explore the optimum conditions on the basis of three-dimensional remediation. Graphite particles with a 5% dosage, resulted from the single-factor experiments, are used in the multi-factor experiments. The results show that the best remediation efficiencies are achieved after 12 d using 0.05 mol L^{-1} citric acid and a voltage gradient of 1.5 V cm^{-1} in three-dimensional electro-kinetic remediation coupled with PRB.

1 Introduction

Soil is a natural resource and an important component of the ecological environment. In recent years, with the development of industrialization, soil contamination has reached at an alarming level worldwide.[1,2] In China, about 1/5 (2×10^7 h m^2) of the cultivated soil area is contaminated by heavy metals such as chromium (Cr), arsenic (As), and lead (Pb). Among these heavy metals, Cr and its compounds are commonly used in metallurgy, electroplating, tanning, and pigment industries. Therefore, during the production and processing of Cr salts, large amounts of wastewater and residues are generated. The improper treatment of Cr residues causes air pollution.[3] Furthermore, hexavalent chromium is highly soluble and causes soil pollution as a result of runoff and infiltration during rainfall. These metals not only deteriorate the soil quality but also affect crops during water uptake and are ultimately a hazard to the human health. Therefore, the remediation of Cr-contaminated soil is a major concern.

Electro-kinetic remediation has been an effective technique to remediate heavy metals from contaminated soil in recent years. It is highly economic as compared to other technologies and has the following characteristics: less labour-intensiveness, simple maintenance, and quick response without the production of secondary pollution. Therefore, more studies have been conducted on electro-kinetic remediation using two-dimensional electrodes across the world, and some European countries have successfully applied it in the field.[4-7] Herein, a new chemical treatment technology called three-dimensional electrode is introduced. It is based on a two-dimensional electrode that is filled with granular materials. These granular materials act as a third electrode/working electrode and have a greater specific surface area as compared to the two-dimensional electrode. Thus, electrochemical reactions are carried on the higher surface area working electrode, which effectively increases the mass transfer effect, current efficiency, and space-time yield.[8-10] Recently, three-dimensional electrodes

[a]State Key Laboratory of Coal Mine Disaster Dynamics and Control, Chongqing University, Chongqing 400044, China. E-mail: litonwei@cqu.edu.cn; j.binquan@cqu.edu.cn

[b]City College of Science and Technology, Chongqing University, Chongqing, 400044, China

[c]Dept. of Construction Management, Chung Hua University, No. 707, Wufu Rd., Sec. 2, Hsinchu 30012, Taiwan. E-mail: ycshiau@chu.edu.tw

[d]Chongqing Solid Waste Management Center, Chongqing 401147, China

† These authors contributed equally to the work.

have been widely used for the treatment of wastewater. Chu *et al.* used them for the removal of COD and colour from wastewater and regarded them as the best technique.[11] In another study, Paidar *et al.* also achieved good results using the abovementioned electrodes for the removal of copper and zinc ions from synthetic solutions.[12] However, their scope is limited for the treatment of contaminated soils.

Electro-kinetic remediation has good results at the laboratory scale as compared to those in field studies. Herein, the electro-kinetic remediation technique coupled with PRB technology is used. Permeable reactive barrier technology is an *in situ* remediation technique that involves the use of tools to dig out soil and then fill a reactive medium to treat the soil and groundwater.[13,14] Currently, the PRB technology is often used with zero-valent iron as the medium to treat contaminated soil and groundwater, and it has been proven as an effective technique to treat several contaminants. The reliability of this technique was proven by Natale *et al.* where they used an activated carbon PRB for the removal of cadmium from a contaminated shallow aquifer.[15] Similarly, Erto *et al.* also used an activated carbon PRB for the *in situ* treatment of aquifers contaminated by chlorinated organic compounds and obtained excellent results.[16] On the other hand, Liu *et al.* achieved good results using natural pyrite as a reactive medium for the treatment of Cr(VI)-contaminated groundwater.[17] Zero-valent iron is used because of its economic value, abundant sources, and high reducibility. It can transform free heavy metal ions (Cr(VI)) into less mobile ions (Cr(III)) or form precipitates.[18,19] Zeolite has good adsorption and ion exchange function; thus, it is often used as a filling material and adsorbent.[20] Basically, electro-kinetic remediation involves the migration and precipitation of ions in the presence of an electric field. During migration, ions come in contact with the PRB and are reduced by zero-valent iron for example Cr(VI) into Cr(III). Moreover, Cr ions are adsorbed by the absorber (zeolite); this will improve the electro-kinetic remediation effect. Therefore, herein, a mixture of zero-valent iron and zeolite is used as the reactive material in the PRB.

The main objective of the current study was to explore the effect of a three-dimensional electrode coupled with a PRB on the treatment of Cr-contaminated sites. In this study, we have discussed (a) the comparison between three-dimensional and two-dimensional electro-kinetic remediation of Cr-contaminated soil; (b) the enhanced utility of a self-made PRB containing a reducer and absorber; and (c) the optimal experimental parameters of three-dimensional electro-kinetic remediation. The leaching toxicity and heavy metal contents before and after electro-kinetic remediation were measured to evaluate the experimental results. X-ray diffraction (XRD) and morphological analysis (Tessier) were used to further analyse the characteristics of the soil samples and explore the removal mechanism of heavy metals.

2 Materials and methods

2.1 Materials

Soil samples were obtained from Minfeng Chemical Industry, Wellhead Industrial Park, Chongqing City, which was chosen

because of the excess of Cr ions in its soil. Samples were obtained from 4 points randomly and sealed in plastic bags, and the sampling depth was about 0–15 cm. Afterwards, the samples were dried at 105 °C for 12 h, ground for 6 h in a roller ball grinder, and sieved through a 200-mesh. Herein, leaching toxicity tests were carried out on the soil samples, and the leachate with the maximum concentration of Cr was selected for further experiments. In addition, the PRB medium contained a filter fabric that was filled with zero-valent iron and zeolite as the reactive medium on an equal mass basis.

2.2 Physical and chemical analysis

2.2.1 Elemental properties of the soil. Semi-quantitative elemental analysis and different phases of the soil samples were measured *via* X-ray fluorescence (XRF, 1800CCDE) (Table 1) and X-ray diffraction (Shimadzu XRD-6000) (Fig. 1), respectively. It can be seen from Table 1, the major elements in the soil sample are O, Ca, and Si, and their cumulative percentage is 73.0084%. The Cr content in the soil is 9.4001%. The major phases were obtained using the MDI Jade software by standardizing the FOM value (<10) as the matching criterion. The analysis result showed that Cr was mostly found as inorganic Cr oxide. Trivalent-chromium (Cr(III)) compounds were observed such as CrOCl. Some compounds have both Cr(III) and Cr(VI); thus, KCr_3O_8 can also be written as $KCr(III)(Cr(VI)O_4)_2$. In addition, the soil sample has some organic compounds of Cr ($C_4H_{16}Cr_2CuN_4O_7$).

2.2.2 Particle size distribution analysis. Soil samples have large particles with an uneven distribution. Therefore, the soil was ground for 4 h and sieved through a 100-mesh. The soil particles were in the range of 1–100 μm, as shown in Fig. 2. It is concluded from the results that D10, D90, and D50 have the particle sizes of 4.71, 137.8, and 40.26 μm, respectively.[21]

2.2.3 Content and leaching toxicity analysis of Cr. The leaching toxicity of Cr(VI) in the original soil sample was extracted in accordance with the HJ/T299-2007 solid waste leaching toxicity of sulfuric and nitric acid method, which was 38.85 mg L^{-1} and greatly exceeded the standard value of solid waste leaching toxicity (GB5085.3-2007). On the other hand, the contents of total Cr and Cr(VI) in the sample were determined by flame atomic absorption spectrophotometry. They were 10512.5 mg kg^{-1} and 423.16 mg kg^{-1}. It can be seen from the

Table 1 Semi-quantitative elemental analysis (%) of the soil sample

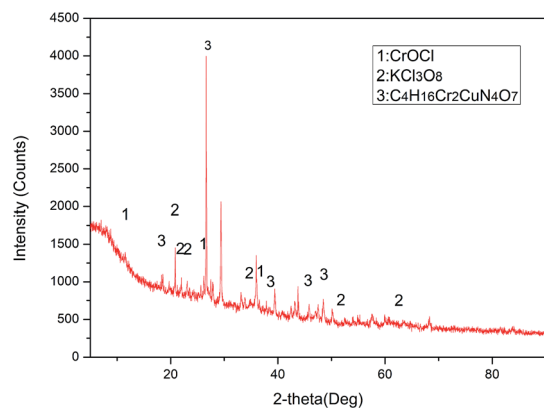| O	Ca	Si	Cr	Fe	Al
48.8788	12.2459	11.8837	9.4001	7.5956	7.3101
Mg	S	K	Na	Ti	Ni
5.7814	1.3629	0.6121	0.3473	0.3001	0.0580
V	Sr	P	Zn	Co	Zr
0.0573	0.0437	0.0404	0.0363	0.0362	0.0101

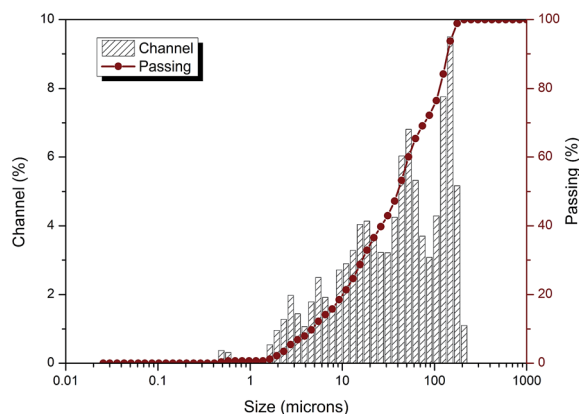Fig. 1 X-ray diffraction pattern of the soil sample.

Fig. 2 Particle size distribution of the soil sample.

results that the Cr content is much higher than the soil residential land secondary standards (GB15618-2008).

2.3 Experimental device

The electro-kinetic remediation experiments were conducted in a rectangular glass reactor with the dimensions of 10 cm × 7 cm × 8 cm (Fig. 3). Activated carbon and graphite worked as the third electrode/particle electrode in the three-dimensional electrode reactor.[22,23] In the current study, graphite particles were used as the third electrode. On the other hand, graphite and stainless-steel plates were used as the anode and cathode electrodes, respectively, and power was supplied *via* an aluminium wire. The experimental sample was Cr-contaminated soil with a 50% moisture content. Potassium chloride (0.1 mol L^{-1}) was used as the electrolytic solution in the anode and cathode regions. In the three-dimensional electro-kinetic remediation coupled with PRB, a 150 g uniform mixture of Cr-contaminated soil and graphite particles were placed in the sample reaction region (Fig. 3(b)) according to its capacity. The sample was evenly divided into three regions, as shown in Fig. 3, T1 (near the anode region), T2 (middle area), and T3 (near the cathode region). According to the literature and experimental conditions, the PRB grid was placed between the T1 and T2 regions, as shown in Fig. 3(b).[24]
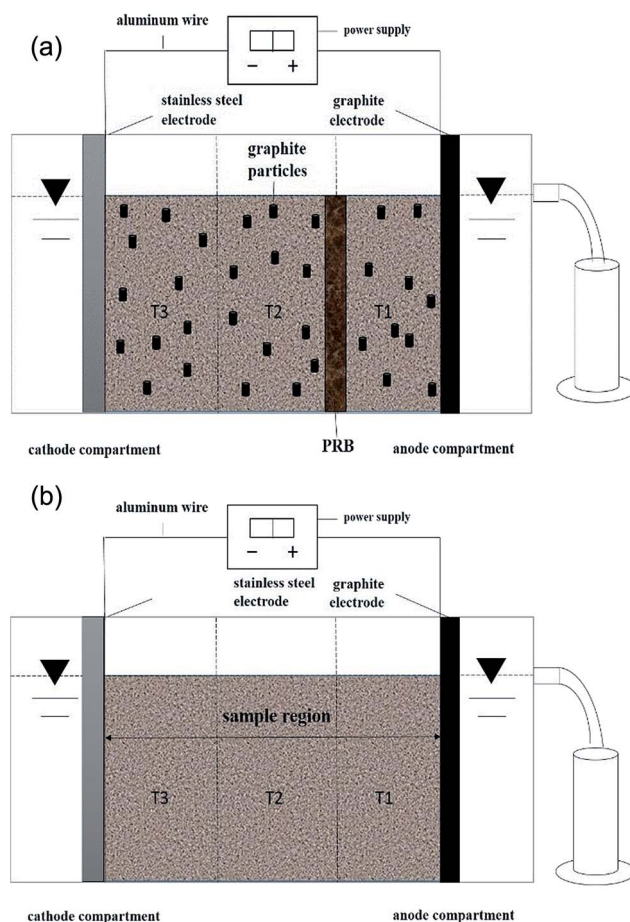

Fig. 3 Electro-kinetic remediation experimental set-up. (a) Two-dimensional electrolytic cell and (b) three-dimensional electrolytic cell coupled with PRB.

2.4 Design of experiment

2.4.1 Design of three experimental conditions. Herein, three electro-kinetic remediation conditions were used: (A) two-dimensional electro-kinetic remediation (EKR), (B) two-dimensional electro-kinetic remediation coupled with PRB (EKR + PRB), and (C) three-dimensional electro-kinetic remediation coupled with PRB (T-EKR + PRB). In the three experiments, remediation was carried out for 5 d at a voltage gradient of 1.5 V cm^{-1}. Moreover, a 5% graphite particle dosage was used in the C experimental condition. The remediation results were compared for the three experimental conditions. The main purpose of this was to determine the remediation effect of the three-dimensional electrode coupled with PRB using the experimental device shown in Fig. 3.

2.4.2 The single-factor experiment. According to the literature, voltage gradient, repair time, graphite particle ratio, and diameters of the particles are important factors that influence the remediation efficiency. In single-factor experiments, the graphite dosage ratio with respect to the soil sample was considered as a variable factor. On the other hand, graphite particle diameter (5 mm × 6 mm), voltage gradient (1.5 V cm^{-1}), and repair time (5 d) were constant factors. The

purpose of the single-factor experiment was to analyse the effect of graphite particle dosage on electro-kinetic remediation with other constant factors, and the experimental layout is presented in Table 2.

2.4.3 Multifactor orthogonal experiment. The optimum dosage ratio was selected on the basis of single-factor experiments and used in orthogonal experiments. Citric acid concentration, voltage gradient, and repair time were the main factors with three levels in the orthogonal experiments (Table 3). The orthogonal experimental layout [L9 (3^4)] is shown in Table 4. Herein, soil samples were treated with citric acid and then placed in the sample region for remediation.

2.5 Calculation of results

To investigate the effectiveness of this technique, Cr leaching toxicity and Cr contents were determined both pre- and post-experiment. Then, the post-experiment results were compared with the pre-experiment results. Chromium removal rate and leaching efficiency were determined using the following formula:

$$y = \frac{U_0 - U}{U_0} \times 100\%$$

Table 2 Single-factor experimental layout

Group	Dosing ratio	Voltage gradient	Repair time
A1	0%	1.5 V cm^{-1}	5 d
A2	5%	1.5 V cm^{-1}	5 d
A3	10%	1.5 V cm^{-1}	5 d
A4	15%	1.5 V cm^{-1}	5 d
A5	20%	1.5 V cm^{-1}	5 d

Table 3 Factors and their levels used in the orthogonal experiments

| Factor | Levels | | |
	1	2	3
Citric acid (CA)	0 mol L^{-1}	0.05 mol L^{-1}	0.1 mol L^{-1}
Voltage gradient (VG)	1 V cm^{-1}	1.5 V cm^{-1}	2 V cm^{-1}
Repair time (RT)	4 d	8 d	12 d

Table 4 Orthogonal experimental layout

Group	Citric acid	Voltage gradient	Repair time
A1	1	1	1
A2	1	3	2
A3	1	2	3
A4	2	1	2
A5	2	2	1
A6	2	3	3
A7	3	1	3
A8	3	2	2
A9	3	3	1

where y is the heavy metal removal rate or leaching efficiency of Cr. U_0 is the content or leaching efficiency in the original soil sample, and U represents the contents or leaching efficiency after electro-kinetic remediation.

## 3 Results and discussion

3.1 Macro phenomena

Similar experimental phenomena were observed under all experimental conditions. In the B and C experimental conditions, more bubbling and a darker yellow colour were observed at the anode region than those under the A experimental condition. The intensity of these phenomena is more prominent under the C experimental condition. The phenomena generated in the three experimental conditions and brief explanations are as follows.

(a) A bubbling phenomenon due to a hydrolysis reaction is observed at the cathode and anode electrodes upon connection with the power source. The following reactions take place as the power is supplied:

Anodic reaction:

$$H_2O - 2e^- \rightarrow 2H^+ + 1/2O_2\uparrow$$
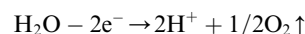
Cathodic reaction:

$$2H_2O + 2e^- \rightarrow 2OH^- + H_2\uparrow$$
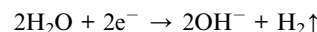
(b) The electrolytic solution changes to yellow brown in the anode region and becomes darker with time; this phenomenon is because of migration of Cr(VI) from the cathode to the anode tank.

(c) During the experiment, the soil within the sample area gradually became compacted and hardened as precipitation occurred due to the presence of OH$^-$ ions in the alkaline environment at the cathode area.

3.2 Three experimental conditions

3.2.1 Change in current with respect to time. The current variations under the three experimental conditions with respect to time are shown in Fig. 4. Generally, the current in a system is related to the amount of charge moving through the sample area in a unit of time. The current variation trend under the three conditions is same: sudden decrease and increase can be seen during the early and middle phase of the experiments, respectively, followed by a gradual decrease in current. The current variations are due to the following reasons: (i) the initial current is higher due to the addition of an electrolytic solution in the anode and cathode regions. With time, the amount of free ions in the electrolytic solution decreases due to their participation or migration towards the sample area; this results in a decrease of current; (ii) the fast migration of H$^+$ ions creates an acidic environment and causes more metal ions to be released; this ultimately increases the current due to presence of a high concentration of free ions; and (iii) the gradual decrease in current is due to precipitation, which lowers the
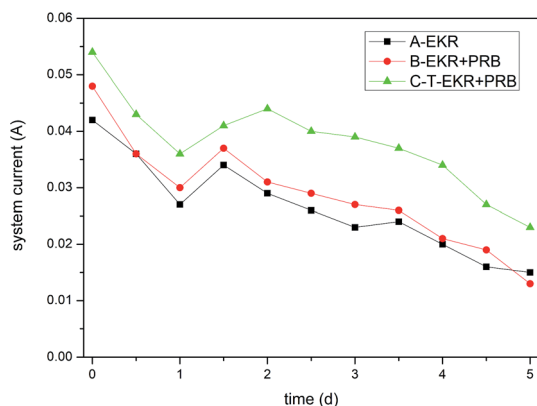
Fig. 4 Change in current *versus* time.

concentration of free ions and increases the resistance. It can also be seen that the C experimental condition has higher current values at all time intervals as compared to A and B, whereas their initial parameters are the same. It can be seen from Fig. 4 that the current variations are nonsignificant between the A and B experimental conditions. This means that the PRB has no significant effect on the current variations. In contrast, the addition of graphite particles as a third electrode increased the current values due to high conductivity of these particles.

3.2.2 Change in pH with respect to time. pH is one of the most important factors that influences the migration of Cr in soil samples. Moreover, the chemical phases, speciation of the minerals phases, and electro-osmosis are significantly affected by the pH in the sample chamber. The pH of 8.84 was observed in the T1, T2, and T3 sample regions before supplying the power. In contrast, the following mechanisms are observed after connecting the power source: hydroxyl ions (OH^-) and hydrogen (H_2) are produced at the cathode, whereas hydrogen ions (H^+) and oxygen (O_2) are produced at the anode due to water electrolysis, as has already been discussed. Therefore, bubbles were generated continuously in the anode and cathode zones. The pH variations can be seen in Fig. 5. Basically, the same pH trend was observed for the three experimental conditions. A gradual increase in pH was observed in the T1–T3

Fig. 5 Change in pH *versus* time.

sample regions. The lower pH at T1 and higher pH at the T3 region are due to the presence of H^+ and OH^- ions, respectively. The H^+ ions are exchanged with cationic contaminants by releasing them from the matrix/soil surface. Moreover, a higher pH gradient is seen in the B and C experimental conditions as compared to that in A. The reason for this phenomenon might be the presence of graphite particles and PRB materials that resulted in the faster migration of ions and intense reactions.[25–27]

3.2.3 Removal rates and leaching efficiency of Cr. Electrokinetic remediation in the three conditions is investigated by the removal rates of Cr(VI) and total Cr and leaching efficiency of Cr(VI) in three sample regions (T1, T2, and T3). The experimental result layout and average values are shown in Table 5. The removal rates and leaching efficiency of Cr(VI) in the three conditions are in following order C > B > A. This indicates that the three-dimensional electro-kinetic remediation coupled with PRB (C), especially the addition of the PRB medium, is effective for the remediation of Cr-contaminated soil. Comparatively, the removal rate (20%) of total Cr is not significant among the three conditions; this is due to the precipitation of $Cr(OH)_3$ during the migration of Cr(III) towards the cathode; this results in a low removal rate of total Cr. As can be seen from Table 5, the removal rate and leaching efficiency of Cr(VI) gradually increased from the T1 to T3 region, and this was because of CrO_4^{2-} anion migration towards the anode during the electro-kinetic remediation process. This phenomenon leads to a higher removal rate of Cr(VI) in the cathode region as compared to that in the anode region.

3.3 Single-factor experiment

3.3.1 Change in current with respect to time. In this section, the effect of graphite particles on current with respect to time has been discussed, as shown in Fig. 6. Initially, current is supplied at the same voltage. The current and graphite particle dosing ratio have strong correlation, and it can be seen (Fig. 6) that the addition of graphite particles has increased the overall current, whereas the other conditions are constant. Therefore, it is concluded that the graphite electrode causes an increase in surface area, electrolysis, and ion exchange reaction under an electric field. The reasons for the current changes have been discussed in the Section 3.2.1.

3.3.2 Removal rates and leaching efficiency of Cr. The average removal rates and leaching efficiency of the T1, T2, and T3 regions in the five groups are shown in Fig. 7. It is concluded from Fig. 7 that the graphite particle ratio has a significant effect on three-dimensional electro-kinetic remediation. The results show that a higher dosage of graphite particles results in a lower removal rate due to the inhibitory effect.

The highest removal rates and leaching efficiency of Cr are observed at the graphite particle dosage of 5%. This means at this level, the Cr(VI) and total Cr contents are lowest in the contaminated soil. In contrast, a higher concentration of graphite (20%) causes the worst experimental result. This is because excess graphite particles may cause blockage of the ion migration paths;
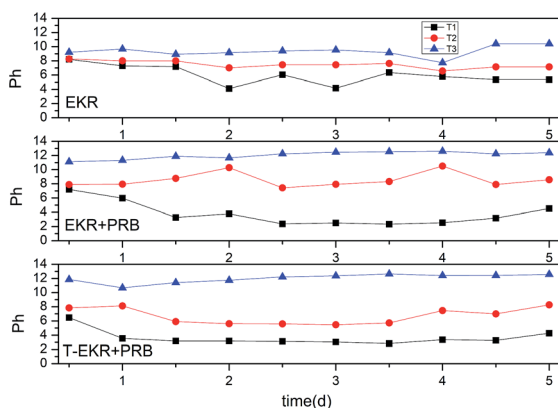
Table 5 Removal rates and leaching efficiency of Cr

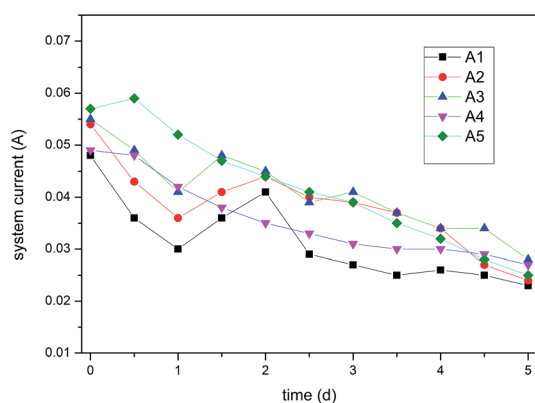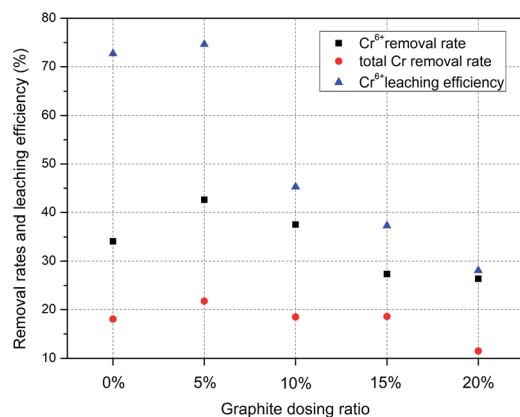| Group	Region	Removal rate of Cr(VI)	Average	Removal rate of total Cr	Average	Leaching efficiency	Average
A-EKR	T1	11.57%	23.51%	21.94%	21.54%	41.79%	53.92%
	T2	16.23%		20.75%		50.09%	
	T3	42.72%		21.94%		69.87%	
B-EKR + PRB	T1	25.35%	40.53%	21.20%	20.16%	62.21%	72.21%
	T2	42.86%		14.95%		72.42%	
	T3	53.37%		24.32%		81.99%	
C-T-EKR + PRB	T1	25.76%	42.99%	20.32%	21.76%	67.79%	75.66%
	T2	44.45%		21.74%		75.05%	
	T3	58.75%		23.22%		84.13%	

Fig. 6 Change in current *versus* time.

Fig. 7 Removal rates and leaching efficiency of Cr in the single-factor experiment.

This results in high resistance, affects current, and ultimately hinders ions movement. Therefore, a high dosing ratio is not proportional to a good remediation effect, and it is concluded that a 5% dosage ratio is optimum for the remediation of Cr-contaminated soil.

3.4 Multi-factor experiment

3.4.1 Change in current with respect to time. Herein, nine experiments were conducted using three factors, each with

different levels (Table 3). The orthogonal experimental layout [L9 (3^4)] is shown in Table 4. It is concluded from Fig. 8 that the initial current values are different because of the different voltage gradients *i.e.* (A2, A6, and A9 = 2 V cm^{-1}), (A3, A5, and A8 = 1.5 V cm^{-1}), and (A1, A4, and A7 = 1 V cm^{-1}). The acidified pre-treatment also increased the current; this was due to the release of more free ions under the acidic environment. The significance of the acidified pre-treatment in the orthogonal experiments is confirmed; hence, this shows its importance in the electro-kinetic remediation of contaminated soil.

3.4.2 Removal rates and leaching efficiency of Cr. In the orthogonal experiment, three-dimensional electro-kinetic remediation coupled with PRB [T-ERK + PRB(C)] was used with the optimum dosage ratio of 5% (achieved from the single-factor experiments). Herein, nine groups were tested, and the average experimental results are shown in Tables 6–8. The results of orthogonal experiments were analysed by range analysis. It can be seen that A8 is the best group having a 50% removal rate of Cr(VI). However, the optimum removal rate of total Cr (23%) and leaching efficiency of Cr(VI) (74%) are noted in group A6. The *R* values show that the three factors have varying influences on the removal rate and leaching efficiency of Cr. Both the removal rate and leaching toxicity of Cr(VI) are influenced by the three factors in following order CA > VG > RT. Therefore, this proves that the acidification pre-treatment of the sample with citric acid has a significant effect on Cr(VI). The underlying reasons for this phenomenon might be the increase
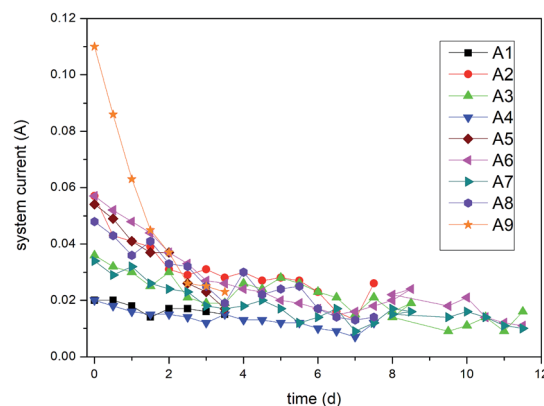

Fig. 8 Change in current *versus* time.

Table 6 Analysis of the Cr(VI) removal rate

Group	CA	VG	RT	Removal rate of Cr(VI)
A1	1	1	1	18.06%
A2	1	3	2	36.70%
A3	1	2	3	46.26%
A4	2	1	2	45.10%
A5	2	2	1	43.34%
A6	2	3	3	49.59%
A7	3	1	3	43.01%
A8	3	2	2	50.31%
A9	3	3	1	44.24%
kj1	33.67	35.39	35.21	
kj2	46.01	46.64	44.04	
kj3	45.85	43.51	46.29	
Optimal levels	CA2	VG2	RT3	
R	12.34	11.25	11.07	
Main sequence	CA > VG > RT			

Table 7 Analysis of the total Cr removal rate

Group	CA	VG	RT	Removal rate of total Cr
A1	1	1	1	12.77%
A2	1	3	2	20.36%
A3	1	2	3	21.53%
A4	2	1	2	17.66%
A5	2	2	1	15.99%
A6	2	3	3	23.81%
A7	3	1	3	19.41%
A8	3	2	2	8.64%
A9	3	3	1	6.94%
kj1	18.22	16.61	11.90	
kj2	19.15	15.39	15.55	
kj3	11.66	17.04	21.58	
Optimal levels	CA2	VG3	RT3	
R	7.49	1.65	9.68	
Main sequence	RT > CA > VG			

Table 8 Analysis of the Cr(VI) leaching efficiency

Group	CA	VG	RT	Leaching efficiency
A1	1	1	1	26.84%
A2	1	3	2	27.72%
A3	1	2	3	66.04%
A4	2	1	2	61.83%
A5	2	2	1	62.79%
A6	2	3	3	74.04%
A7	3	1	3	57.42%
A8	3	2	2	70.06%
A9	3	3	1	66.09%
kj1	40.20	48.70	51.90	
kj2	66.22	66.30	53.20	
kj3	64.52	55.95	65.83	
Optimal levels	CA2	VG2	RT3	
R	26.02	17.60	13.93	
Main sequence	CA > VG > RT			

3.5 Removal mechanisms of Cr

3.5.1 Phase changes. Based on the abovementioned discussion, the samples with the best experimental results were subjected to XRD analysis. The existence of Cr in the organic form ($C_8H_{24}CrN_2O_4$) is confirmed by the XRD pattern, as shown in Fig. 9. However, CrOCl and KCr_3O_8 are not detected by XRD. Basically, the XRD results show that the soil samples, which are remediated by the T-EKR + PRB system, have fewer phases as compared to the original soil samples phases; this indicates that more contaminants are dissolved, and electro-kinetic remediation is suitable for water-soluble and acid-extractable ions. Hence, its effect on the removal of organic and residual Cr is not significant. Therefore, this proves that the present study is useful for the removal of inorganic Cr.

3.5.2 Changes in morphology. Chromium in soil shows different morphologies by dissolution, cohesion, precipitation, complexation, and other reactions. Thus, the migration and transformation mechanisms are different for different morphologies of Cr in electro-kinetic remediation. The samples were analysed using the Tessier method before and after the treatment, and the results are shown in Fig. 10. Most of the Cr in the soil existed with the residual form. Obviously, the exchangeable and carbonate fraction in the sample decreased
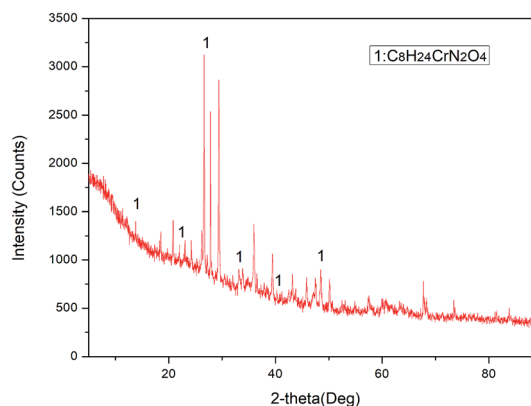
in pollutant desorption from the surface of the soil matrix and the enhancement of the complex reaction on the surface of the PRB materials with the action of acidification pre-treatment. However, in the case of total Cr, the factor RT has a greater effect on the removal rate than VG followed by CA. This indicates that the total Cr is significantly affected by the repair time since more Cr participates in the reaction with time and results in a decline of the removal rate. From the K values, the best removal rate and leaching efficiency of Cr(VI) are achieved at the VG2 level, and VG3 is considered the best voltage gradient for the removal of total Cr. However, the difference among VG1, VG2, and VG3 is non-significant; thus, VG2 is selected as the best level for voltage gradient. The optimal levels for repair time and concentration of acidification pre-treatment are RT3 and CA2, respectively. Therefore, the optimum levels are obtained with the citric acid concentration of 0.05 mol L^{-1}, voltage gradient of 1.5 V cm^{-1}, and repair time of 12 d in this remediation system.

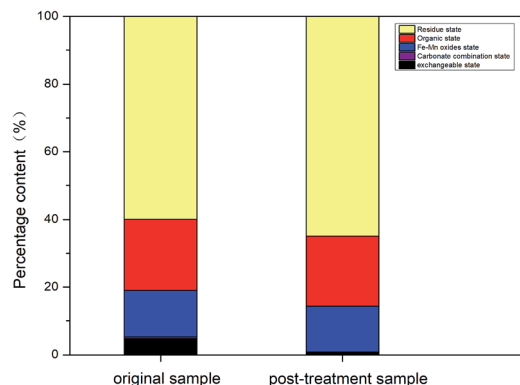**Fig. 9** XRD analysis of the soil samples after remediation.

Fig. 10 Results of Tessier morphological analysis.

significantly after remediation. This indicates the reduction of the acid extractable Cr. The results further verify that the three-dimensional electrode coupled with PRB is very effective to deal with acid-extractable heavy metals in soil; however, the oxidation state and organic matter are not affected. Furthermore, the residual form of Cr is present in a higher proportion, but it cannot be released due to its high stability. Therefore, its impact on the environment is relatively small.

From the abovementioned analysis, macro-phenomena (e.g. bubbling and precipitation), system current, and pH value were observed at regular intervals. The experimental results were analysed using the removal rates and leaching efficiency. The removal mechanisms contain the following steps: (a) the remediation is mainly focused on acid-extractable Cr. (b) Acid-extractable Cr(VI) is reduced by PRB medium and reduced Cr(III) forms complexes with Fe. (c) Moreover, the addition of a certain amount of graphite particles enhances the reaction efficiency, and more extractable Cr(VI) is reduced. (d) Higher precipitation of Cr [Cr(OH)$_3$] is experienced in the cathode region because of high pH. Hence, the remediation of total Cr is not ideal in this region. (e) In the acidification-enhanced experiments, the addition of organic acids not only plays an important role in neutralizing the pH of the cathode region but also accelerates the release of ions.[28,29] Our results are supported by Yang Jiewen,[30] who have also concluded that iron oxide and organic acids play a vital role in reducing the toxicity of Cr(VI) and can be used for the remediation of Cr from soils.

4   Conclusion

The soil used in the experiments had higher Cr contents as compared to residential land secondary standards (GB15618-2008), and its leaching toxicity also exceeded the standard value of the solid waste leaching toxicity (GB5085.3-2007). The following conclusions were made from this study: (1) three electro-kinetic experiments were carried out to determine their effectiveness for Cr remediation. The coupling experiments using the PRB (EKR + PRB, T-EKR + PRB) had better results than the traditional two-dimensional electro-kinetic remediation. In contrast, the maximum efficiency was observed in the three-dimensional electro-kinetic experiment coupled with the PRB

(T-EKR + PRB); (2) the graphite particle dosage ratio of 5% had a more reliable effect as compared to the higher dosages, which had inhibitory effects on the remediation process; (3) in the multi-factor orthogonal experiments, Cr(VI) and total Cr remediation were greatly influenced by acidification pre-treatment and repair time, respectively, based on the analysis of individual factors. Moreover, the orthogonal multi-factor experiment results showed that the best results were achieved using citric acid at a concentration of 0.05 mol L^{-1}, voltage gradient of 1.5 V cm^{-1}, and repair time of 12 d in the T-EKR + PRB system; and (4) finally, three-dimensional electro-kinetic remediation coupled with PRB had a good influence on exchangeable and acid extractable-Cr rather than that on organic and residual Cr. Thus, this technique can be recommended for the remediation of Cr-contaminated soils.

Conflicts of interest

There are no conflicts to declare.

References

1 Z. Yao, J. Li, H. Xie and C. Yu, *Procedia Environ. Sci.*, 2012, **16**, 722–729.
2 T. Yang, L. Meng, S. Han, J. Hou, S. Wang and X. Wang, *RSC Adv.*, 2017, **7**, 34687–34693.
3 Z. Wanliang, Z. Manli, C. Hongying, L. Anping, Y. Dongxia and Z. Xuemei, *Procedia Environ. Sci.*, 2016, **31**, 247–254.
4 D. Li, D. Sun, S. Hu, J. Hu and X. Yuan, *Chemosphere*, 2016, **144**, 1823–1830.
5 T. Huang, D. Li, L. Kexiang and Y. Zhang, *Sci. Rep.*, 2015, **5**, 15412.
6 A. T. Yeung and Y. Y. Gu, *J. Hazard. Mater.*, 2011, **195**, 11–29.
7 X. Huang, T. Huang, S. Li, F. Muhammad, G. Xu, Z. Zhao, L. Yu, Y. Yan, D. Li and B. Jiao, *Ceram. Int.*, 2016, **42**, 9538–9549.
8 D. Li, Y.-Y. Niu, M. Fan, D.-L. Xu and P. Xu, *Sep. Purif. Technol.*, 2013, **120**, 52–58.
9 K. Grace Pavithra, P. Senthil Kumar, F. Carolin Christopher and A. Saravanan, *J. Phys. Chem. Solids*, 2017, **110**, 379–385.
10 Y. Zhang, T. Huang, X. Huang, M. Faheem, L. Yu, B. Jiao, G. Yin, Y. Shiau and D. Li, *RSC Adv.*, 2017, **7**, 27846–27852.
11 H. Q. Chu, Z. Wang and Y. Liu, *J. Environ. Chem. Eng.*, 2016, **4**, 1810–1817.
12 M. Paidar, K. Bouzek, M. Laurich and J. Thonstad, *Water Environ. Res.*, 2000, **72**, 618–625.
13 P. Oprčkal, A. Mladenovič, J. Vidmar, A. Mauko Pranjić, R. Milačič and J. Ščančar, *Chem. Eng. J.*, 2017, **321**, 20–30.
14 H. Pullin, R. A. Crane, D. J. Morgan and T. B. Scott, *J. Environ. Chem. Eng.*, 2017, **5**, 1166–1173.
15 F. Di Natale, M. Di Natale, R. Greco, A. Lancia, C. Laudante and D. Musmarra, *J. Hazard. Mater.*, 2008, **160**, 428–434.
16 A. Erto, I. Bortone, A. Di Nardo, M. Di Natale and D. Musmarra, *J. Environ. Manage.*, 2014, **140**, 111–119.
17 Y. Y. Liu, H. Y. Mou, L. Q. Chen, Z. A. Mirza and L. Liu, *J. Hazard. Mater.*, 2015, **298**, 83–90.

18 A. Galdames, A. Mendoza, M. Orueta, I. S. de Soto García, M. Sánchez, I. Virto and J. L. Vilas, *Resource-Efficient Technologies*, 2017, **3**, 166–176.

19 Y. Li, T. Li and Z. Jin, *J. Environ. Sci.*, 2011, **23**, 1211–1218.

20 M. M. Arimi, *Prog. Nat. Sci.: Mater. Int.*, 2017, **27**, 275–282.

21 R. Chen, Y. Li, R. Xiang and S. Li, *Constr. Build. Mater.*, 2016, **123**, 120–126.

22 B. Shen, X.-h. Wen and X. Huang, *Chem. Eng. J.*, 2017, **327**, 597–607.

23 H. I. Gomes, C. Dias-Ferreira and A. B. Ribeiro, *Chemosphere*, 2012, **87**, 1077–1090.

24 J. Zhang, C. Zhang, G. Wei, Y. Li, X. Liang, W. Chu, H. He, D. Huang, J. Zhu and R. Zhu, *J. Colloid Interface Sci.*, 2017, **500**, 20–29.

25 M. Szabó, J. Kalmár, T. Ditrói, G. Bellér, G. Lente, N. Simic and I. Fábián, *Inorg. Chim. Acta*, 2017, DOI: 10.1016/j.ica.2017.05.038.

26 D. Pei, C. Xiao, Q. Hu and J. Tang, *Procedia Environ. Sci.*, 2016, **31**, 725–734.

27 N. D. Mu'azu, M. H. Essa and S. Lukman, *J. King Saud Univ., Eng. Sci.*, 2016, DOI: 10.1016/j.jksues.2016.12.002.

28 R. Fu, D. Wen, X. Xia, W. Zhang and Y. Gu, *Chem. Eng. J.*, 2017, **316**, 601–608.

29 G. Li, X. Yang, L. Liang and S. Guo, *Arabian J. Chem.*, 2017, **10**, S539–S545.

30 J. Yang, L. Zhong and L. Liu, *J. Environ. Chem. Eng.*, 2017, **5**, 2564–3256.